IHJPAS.37 (2) 2024
Ibn Al-Haitham Journal for Pure and Applied Sciences
Journal homepage: jih.uobaghdad.edu.iq
PISSN: 1609-4042, EISSN: 2521-3407

Synthesis, Characterization and Determination Antioxidant Activities for New Azo Dyederived from Sulfamethoxazole and Some Metal Ion Complexes

Amnah Mahdi Abdullah[1*], Abbas Ali Salih Al-Hamdani[2] and Wail Al Zoubi[3]

[1,2] Department of Chemistry, College of Science for Women, University of Baghdad, Baghdad, Iraq.
[3] School of Materials Science and Engineering,Yeungnam University, Gyeongsan 712-749, South Koria.
*Corresponding Author.

Received:7 February 2023 Accepted:2 April 2023 Published:20 April 2024

doi.org/10.30526/37.2.3279

Abstract

Diazotization reaction between 1-(2,4,6-trihydroxy-phenyl)-ethanone and diazonium salts produced the ligand 4-(3-Acetyl-2,4,6-trihydroxy-phenylazo)-N-(5-methyl-isoxazol-3-yl)-benzenesulfonamide, which in turn reacted with the metal ions (Ni^{2+}, Zn^{2+}, Pd^{2+} and Pt^{4+}) forming stable complexes with Octahedral geometry suggest of (Ni^{2+} and Pt^{4+}), Zn^{2+} complex Tetrahedral and Pd^{2+} complex Square planer. The creation of such complexes was detected by employing spectroscopic means involving ultraviolet-visible, which proved the obtained geometries; FT-IR confirmed the formation of the azo group and the coordination with metal ions through it. Thermogravimetric analysis studies demonstrated the coordination of water residues (aqua or hydrate) with metal ions inside the coordination sphere, as well as used curve DSC to calculate the thermodynamic parameters ΔH, ΔS, and ΔG. Moreover, element microanalysis and atomic absorption gave corresponding outcomes with theoretically counting outcomes. Neuclearmagnatic resonances for ^{1}H and ^{13}C, chlorine atoms, and magnetic moment quantifications also indicate the formation of azo dye ligand. The ligand and new complexes showed antioxidant abilities to scavenge free radicals.

Keywords: Antioxidant, mass spectroscopy, azo dye, 1-(2,4,6-trihydroxy-phenyl)-ethanone, thermal analysis.

1. Introduction

Until the middle of the 19th century, all coloring materials were supplied from natural sources such as inorganic dyes [1]. As for natural organic dyes, they also have an ancient history of use, especially in Tissues dyeing [2]. Heterogeneous azo compounds, in particular, won a wide area in several fields because they contain more than one active group that has the ability to form complexes of colored aggregates, which facilitates the spectroscopic determination of very small concentrations of metal ions using the visible-ultraviolet spectra [3-5]. This led to the emergence of new dyes, and Kekule's discovery of the molecular structure of benzene in 1865 had a great impact on the development of dyes until the beginning of the twentieth century [6,7].

Thus, natural dyes were replaced by synthetic dyes [8]. Azo dyes are organic substances consisting of two organic groups linked through coupling reactions with an azo group to give colored compounds that are absorbed in the visible and ultraviolet regions [9-12]. Azo dyes are considered the most significant group within organic dyes, which are prepared industrially and can add colors to fibers [13]. They contain an azo group – N = N – as nitrogen atoms are linked to carbon atoms with Sphybridization and at least one carbon atom is connected to a ring (usually benzene or naphthalene derivatives) or polycyclic such as (Pyrazolone or Thiazole) [14]. Studies have shown that these compounds represent essential drugs, as they were found to have properties that inhibit the growth of bacteria [15-17]. Due to the importance of these compounds, the current research included the preparation and identification of a new azo dye derived from 1-(2,4,6-Trihydroxy-phenyl)-ethanone and sulfamethoxazole. This work aims to synthesize new metal ions complexes (Ni^{2+}, Zn^{2+}, Pd^{2+} and Pt^{4+}) from azo ligand H_3L as well as characterization with spectroscopic analysis and studying thermal decomposition and thermal stability by using DSC and TGA curve. This study uses curve DSC to calculate the thermodynamic parameters ΔH, ΔS and ΔG then antioxidant activity of these compounds against the DPPH radicals and compare to those of the natural antioxidant gallic acid.

2. Materials and Methods

Materials have been obtained from the trading suppliers (Sigma Aldrich, Merck, and others). The eurovectormodel EA/3000, singleV_3O, has been employed to achieve (C.H.N.S and O). Mineral-ions have determined as M-O using a gravimetric-approaches. Molar conductivity has been estimated by operating Conduct meter W-T-W, at room temperature, 1×10-3 M. DMSO has been employed as solvent. Mass spectra for substances have been collected using mass spectrometry (MS) Q-P-50-A-D-I Analysis Shimadzu QP (E170Ev) -2010-Pluss spectrometer. The UV-visible absorption spectra were obtained using a UV-1800 Shimadzu spectrophotometer. The Brucker (400 MHz) spectrometer was used to obtain the ^{1}H and ^{13}C NMR spectra. The IR Prestige-21 was used to investigate the Fourier transform infrared (FTIR) spectra, where the device was used Shimadzu 4000-200 cm^{-1} by CsI and Bruker 4000-500 cm^{-1} by KBr. The F.A.A. determined the metal percentage. The balancing susceptibility model MSR-MKI utilized magnetic characteristics. Perkin-Elmer Pyris Diamond DSC/TGA was used for all prior sorts of thermal analysis. The chlorine content of the prepared complexes was measured using Moore's method 686-titro processor-665. The magnetic sensitivity was also measured using the Magnetic Susceptibility Balance Model (MSB-MKI) device.

2.1 Synthesis of azo dye ligand [4-(3-Acetyl-2,4,6-trihydroxy-phenylazo)-N-(5-methyl–isoxazol-3-yl)–benzenesulfonamide]

Sulfamethoxazole (1 g, 3.948 mmol) was dissolved in (2 mL of HCl and 10 mL of ethanol) at 0-5°C, gradually added (10%, 1 g, 14.49 mmol) $NaNO_2$ stirred for approximately 45 minutes, then, the (0.663 g, 3.948 mmol) of 1-(2,4,6-Trihydroxy-phenyl)-ethanone dissolved in 15 mL of ethanol was added. The change to a dark-colored solution was observed after stirring for 30 minutes. This product is collected after being filtered and dried. Its melting point was (146-148)°C and the color of precipitate was orange, its yield was 93%. **Scheme 1** shows the formation of the ligand azo dye. The ligand showed bands at 3503, 3281,3014, 2979, 1635 and (1088-1015) cm^{-1} that were ascribed to the ν (OH) phenolic, ν (NH), ν (C-H) aromatic,ν (C-H) aliphatic,ν (C=O) and ν (SO_2). The infrared spectrum of the ligand showed a medium-intensity

stretch band at a frequency of 1485 cm^{-1}, which was attributed to the vibrational frequencies of the double bond N=N. The UV-Vis spectrum exhibits strong absorbance at (286 nm, 34965.04 cm^{-1}), ascribed to the $\pi \longrightarrow \pi^*$ transition and peak at (392 nm, 25510.20 cm^{-1}) attributed to the $n \longrightarrow \pi^*$ transition peak [18]. The ^{1}H-NMR and ^{13}C-NMR spectra of Newazo, which can be seen in **Figure 1**, demonstrate the chemical shifts of these spectra. ^{1}H-NMR (DMSO-d6, ppm):1.92 ppm (3H,s, CH_3), 2.08 ppm (3H,s, CH_3CO), CH_3,6.43 ppm, (1H, s, C-H) isoxazole ring [The rest of the ^{1}HNMR signals are arranged in this manner, 6.77 ppm, (1H,s, CH aromatic) beside OH, (7.26-8.1) ppm (4H, dd, aromatic), 8.11 ppm (1H,s, NH), 8.74 ppm (1H)S, (OH) phenolic beside (N=N), 8.75 ppm, (1H)S (OH) phenolic beside (N=N) and it belongs to NH, (OH) phenolic beside $COCH_3$. ^{13}C-NMR: 33.62(C_1), 49.71(C_{18}), 106.90(C_{13}), 118.20(C_3), 127.48(C_{15}), 132.21(C_{11}), 137.27(C_9), 145.00(C_7), 148.96(C_{10}), 155.15(C_6), 157.23(C_5), 165.30(C_4), 169.75(C_{16}), 172.24(C_8), 178.10(C_{12}), 181.97(C_2), 189.75(C_{14}) and 196.20 (C_{17}) [19,20]. LC-Mass spectrum was tested using an LC-Mass device; this approach is one of the most essential approaches in characterization and complementary to the rest of the approaches by which the molecular weight of the compound is estimated according to the relation (m/z). Mass information of the ligand in **Scheme 1** shows the fragmentation pattern and the extracted mass for each pattern. It can be clearly observed the molecular ion peak $[M]^{+}$ for the fragment $C_{14}H_{10}N_2O_6S^{\bullet+}$ and its relative abundance of about 66% in **Figure 2**, in addition to other abundances for the rest of peaks including $C_8H_8N_2O_4^{\bullet+}$, $C_6H_4O_2S^{\bullet+}$ and $C_4H_4N_2O^{\bullet+}$, corresponded the next abundances: 47%, 33% and 79% respectively [21].

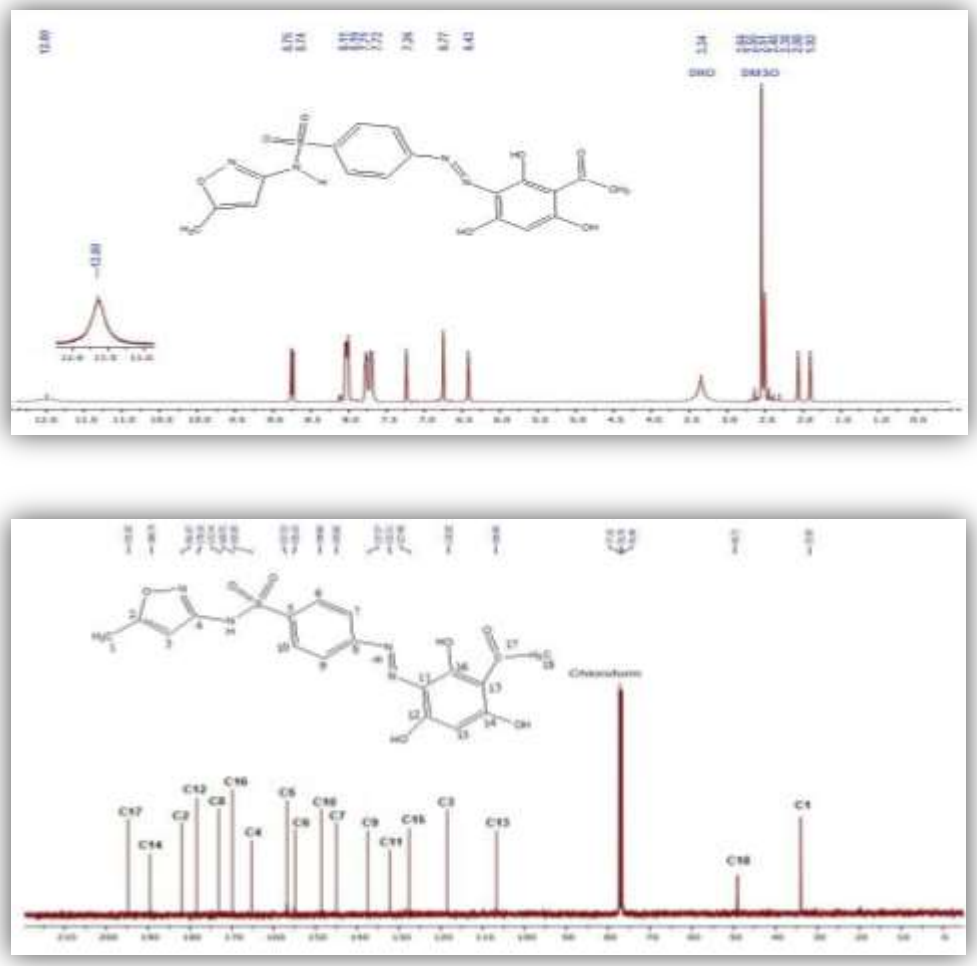

Figure 1. The ^{1}H and ^{13}C-NMR spectra of ligand (H_3L).

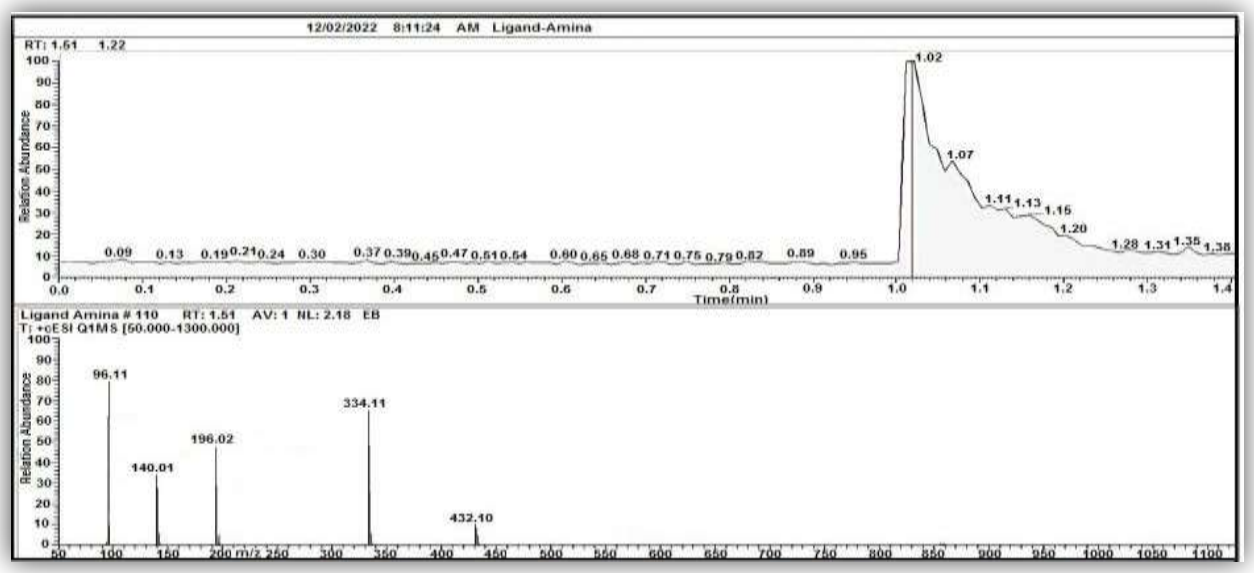

Figure 2. Mass spectrum of ligand.

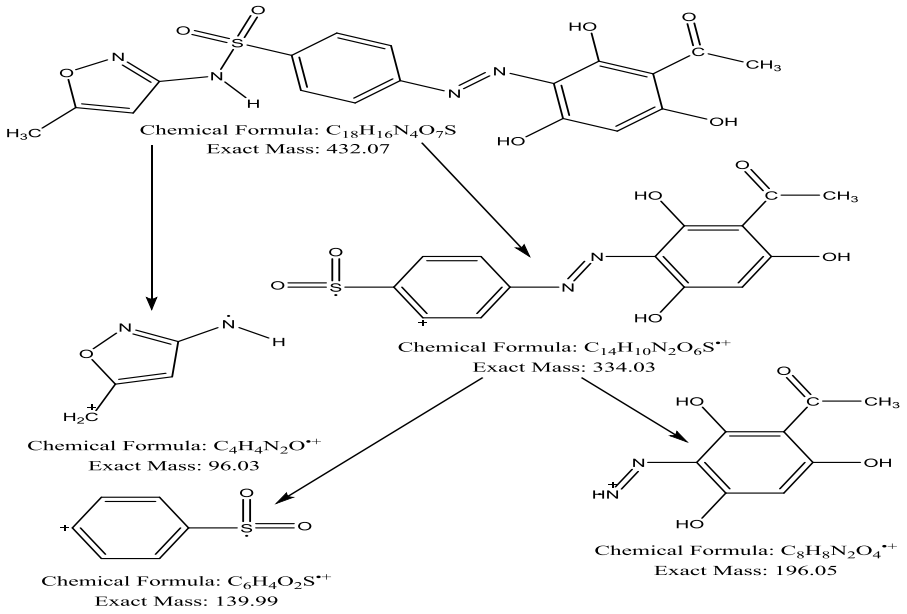

Scheme 1. Pattern of fragmentation of ligand.

2.2 General approach for complexes synthesis

The metal salt (1 mmol) of [0.1979 g $NiCl_2.6H_2O$, 0.1364 g $ZnCl_2$, 0.17742 g $PdCl_2$ and 0.5178 g $H_2PtCl_6.6H_2O$] was dissolved in 15 mL of hot ethanol. Then (0.432 g, 1 mmol) of azo dye in 15 mL of hot ethanol was added drop by drop. The mixture washeated under reflux for 6 hours up to 40-50 °C. The solid complexes were separated and any non-apostate ingredients are removed by immersing them shortly in the hot ethanol. The complexes were collected, dried and weighed. **Schem 2** shows the formation of the metal ions complexes.

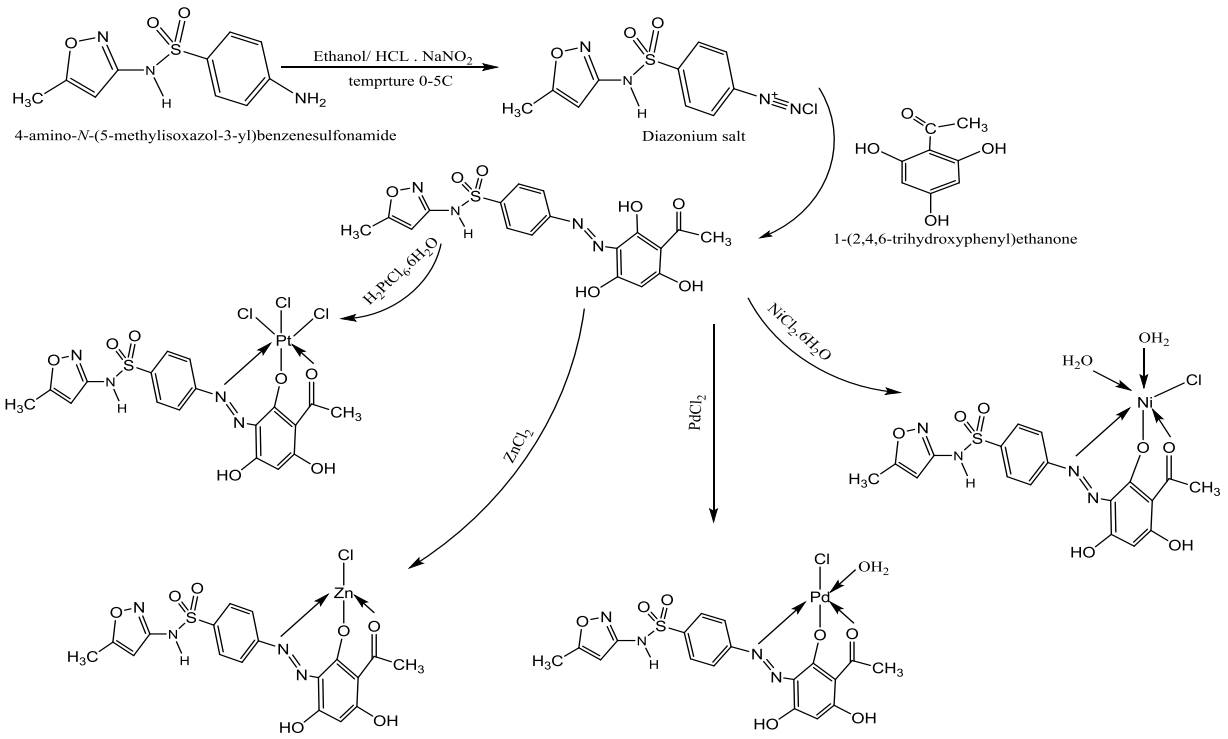

Scheme 2. Formation for ligand and their metal complexes.

3. Results and Discussion

3.1 Physical and analytical data for ligand and the synthesized complexes

Reactions of metal salts with ligands gave the synthetic complexes, as shown in **Scheme 1**. The results of the elemental analysis demonstrate 1:1 M: L stoichiometry for all complexes. The elemental analysis results were compatible with the theoretical calculated results, as denoted in **Table 1**.

Table 1. Some physical propertiesand element micro analysis studies of ligand and complexes.

Compounds formula M.wt	Micro elemental analysis (Found) and Calculated %								
	C	H	N	O	S	M	Cl	Color	m.p °C
H_3L= $C_{18}H_{16}N_4O_7S$ = 432	(50.55) 50.00	(4.01) 3.72	(14.00) 12.96	(25.10) 25.90	(6.70) 7.42	--	--	Orange	146-148
$C_{18}H_{19}N_4O_9SClNi$ = 561.1934	(37.77) 38.49	(4.09) 3.38	(10.96) 9.98	(26.01) 25.66	(6.05) 5.70	(11.09) 10.46	(7.03) 6.33	Brown	196 d
$C_{18}H_{17}N_4O_8SClZn$= 549.909	(40.01) 39.28	(3.00) 3.09	(11.61) 10.18	(22.66) 23.28	(5.62) 5.82	(11.10) 11.89	(6.00) 6.46	Brown	259 d
$C_{18}H_{15}N_4O_7SClPd$=572.92	(38.65) 37.68	(2.09) 2.64	(10.67) 9.77	(18.91) 19.54	(6.09) 5.60	(16.69) 18.58	(7.08) 6.19	Light Brown	220 d
$C_{18}H_{15}N_4O_7SCl_3Pt$ = 732.578	(30.01) 29.48	(2.41) 2.05	(8.01) 7.64	(15.21) 15.29	(5.05) 4.37	(25.67) 26.63	(13.69) 14.54	Dark Brown	186 d

d=decompose.

3.2 The UV-Vis studies of the complexes

The UV-Vis spectrum exhibits the electronic transition of Pt^{4+}complex show in **Figure 4** depicts a peak of (288, 375, 615, 632 and 680) nm assigned to π→ π*, n→ π*, $^1A_1g \rightarrow {}^1T_1g$, $^1A_1g \rightarrow {}^1T_2g$ and $^1A_1g \rightarrow {}^3T_2g$ respectively which indicative of a Octahedral geometry, it has a magnetic moment of diamagnatic. The Ni^{2+} complex show in **Figure 3** exhibited peaks of (220, 270, 418, 614, 730 and

840) nm ascribed to the π→π*, n→π*, C.T M→L, $^3A_1g \rightarrow {}^3T_2g_{(F)}$, $^3A_1g \rightarrow {}^3T_1g_{(F)}$ and $^3A_2g \rightarrow {}^3T_1g_{(P)}$ respectively is in good agreement with prior work on octahedral geometry, it has a magnetic moment of 2.13 [22].

The electronic absorption of Zn^{2+}complexe exhibited peaks of (263, 368 and 447) nm ascribed to the π →π*,n→π* and C.TM→L respectively which is indicative of a Tetrahedral geometry, it has a magnetic moment of diamagnetic [23].

The Pd^{2+}complexe exhibited peaks at (262, 363, 421, 700 and 804) nm ascribed to the π→ π*, n→ π*, C.TM→L, $^1A_1g \rightarrow {}^1B_1g$ and $^1A_1g \rightarrow {}^1A_2g$ respectively is in good agreement with prior work on Squar planer geometry it has a magnetic moment of diamagnetic [24]. **Table 2** displays the electronic assignmentfor metal complexes.

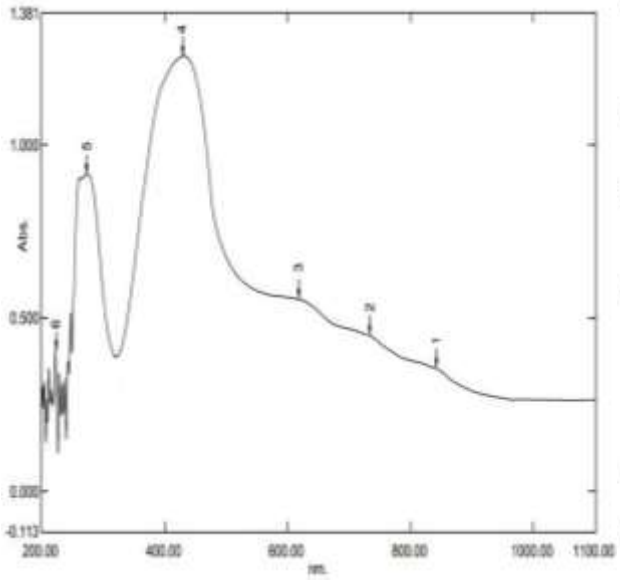

Figure 3. The UV-Vis spectrum of Ni-complex.

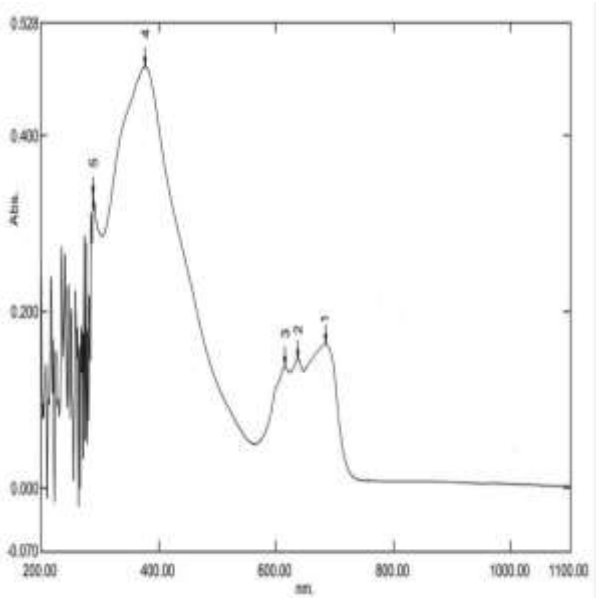

Figure 4. The UV-Vis spectrum of Pt-complex**.**

Table 2. The UV-Vis spectra, magnetic moments and molar conductivity for metal complexes.

Compound	λ nm	ύ cm^{-1}	Abs	ε_{max} L $mol^{-1}cm^{-1}$	Assignment	μ_{eff} (B.M)	ΛmS. cm^2. Mol^{-1}
$[Ni(H_2L)(H_2O)_2Cl]$	220	45454.55	0.400	4000	π→π*	2.13	13
Octahedral	270	37037.04	0.950	9500	n→π*		
	418	23923.45	1.238	12380	C.T M→L		
	614	16286.65	0.550	5500	$^3A_1g \rightarrow {}^3T_2g_{(F)}$		
	730	13698.63	0.485	4850	$^3A_1g \rightarrow {}^3T_1g_{(F)}$		
	840	11904.76	0.380	3800	$^3A_2g \rightarrow {}^3T_1g_{(P)}$		
$[Zn(H_2L)(H_2O)Cl]$	263	38022.81	1.400	14000	π→π*	diamagnatic	16
Tetrahedral	368	27173.91	1.063	10630	n→π*		
	447	22371.36	1.581	15810	C.T M→L		
$[Pd(H_2L)Cl]$	262	38167.942	0.540	5400	π→π*	diamagnatic	13
Square planer	363	7548.2123	0.355	3550	n→π*		
	421	752.97142	0.610	6100	C.T M→L		
	700	85.711243	0.038	380	$^1A_1g \rightarrow {}^1B_1g$		
	804	7.81	0.040	400	$^1A_1g \rightarrow {}^1A_2g$		
$[Pt(H_2L)Cl_3]O$	288	34722.22	0.340	3400	π→π*	diamagnatic	20
Octahedral	375	26666.66	0.485	4850	n→π*		
	615	16260.16	0.144	1440	$^1A_1g \rightarrow {}^1T_1g$		
	632	15822.78	0.160	1600	$^1A_1g \rightarrow {}^1T_2g$		
	680	14705.88	0.180	1800	$^1A_1g \rightarrow {}^3T_2g$		

3.3 The LC-Mass spectrum of complexes

The LC-Mass spectrum of the products were tested using LC-Mass device, this approach is one of the most essential approaches in characterization and complementary for the rest approaches by which the molecular weight of the compound is estimated according to the relation (m/z). For $[Ni(H_2L)(H_2O)_2Cl]$, **Figure 5** and **Scheme 3**, it can also be detected the molecular ion peak (M^+) at 559.99 m/z with the relative abundance of 10% and following patterns: $C_{18}H_{15}ClN_4NiO_7S^+$, $C_{14}H_{10}ClN_2NiO_4^{\bullet+}$, $C_6H_6ClN_2NiO_2^{\bullet+}$, $C_4H_4N_2O_3S^{\bullet+}$ and $C_8H_7O_2^+$, which corresponded to 523.97 m/z, 362.97 m/z, 230.95 m/z, 159.99 m/z and 135.04 m/z respectively [25].

For $[Pd(H_2L)Cl]$ complex in **Figure 6** and **Scheme 4** illustrate the following fragments: (M^+) at 571.94 m/z with the relative abundance of 21%, $C_{18}H_{15}N_4O_7PdS^{\bullet+}$, $C_5H_6O_3Pd^{\bullet+}$, $C_6H_5NO_2S^{\bullet+}$, $C_3H_4N_2O^{\bullet+}$, and $C_4H_4NO^+$ that correspond to 536.97 m/z, 219.93 m/z, 155.00 m/z, 84.03 m/z and 82.03 m/z respectively [26]. Finally, $[Pt(H_2L)Cl_3]$ complex in **Figure 7** and **Scheme 5** illustrate the following fragments: (M^+) at 730.94 m/z with the relative abundance of 29%, $C_{18}H_{15}N_4O_7PtS^+$, $C_5H_6O_3Pt^{\bullet+}$, $C_6H_5NO_2S^{\bullet+}$, $C_3H_4N_2O^{\bullet+}$and $C_4H_4NO^+$ that correspond to 626.03 m/z, 309.00 m/z, 155.00 m/z, 84.03 m/z and 82.03 m/z respectively [27].

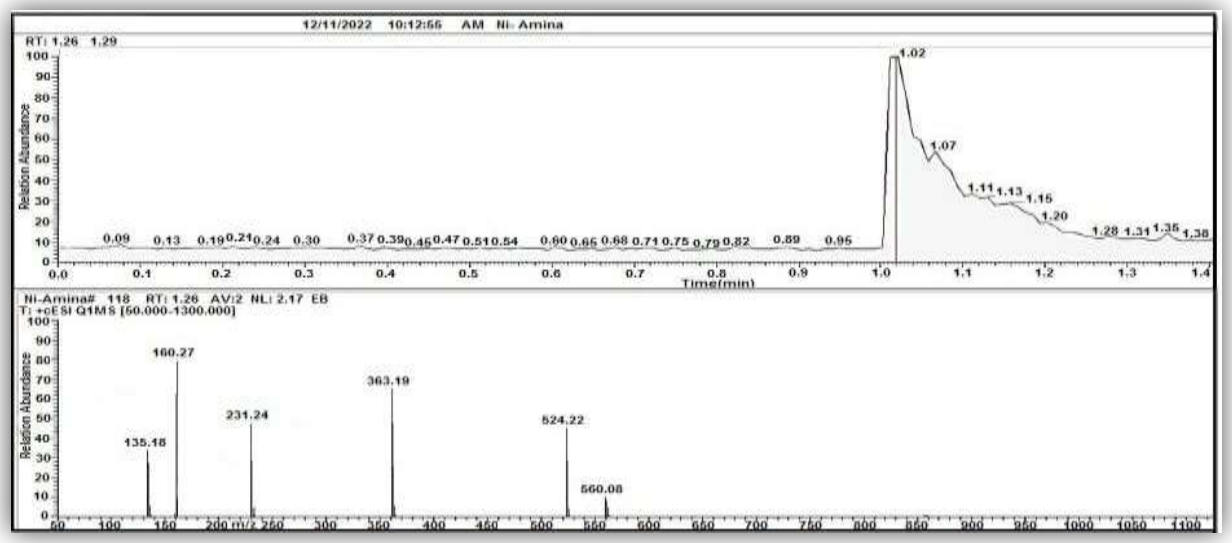

Figure 5. Mass spectrum of Ni-complex.

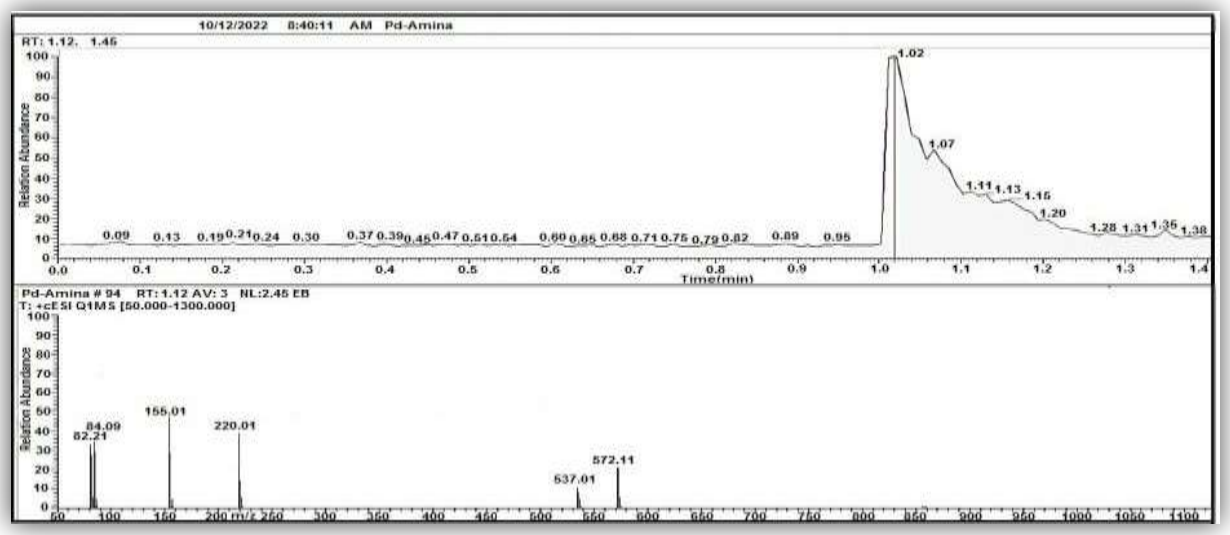

Figure 6. Mass spectrum of Pd-complex.

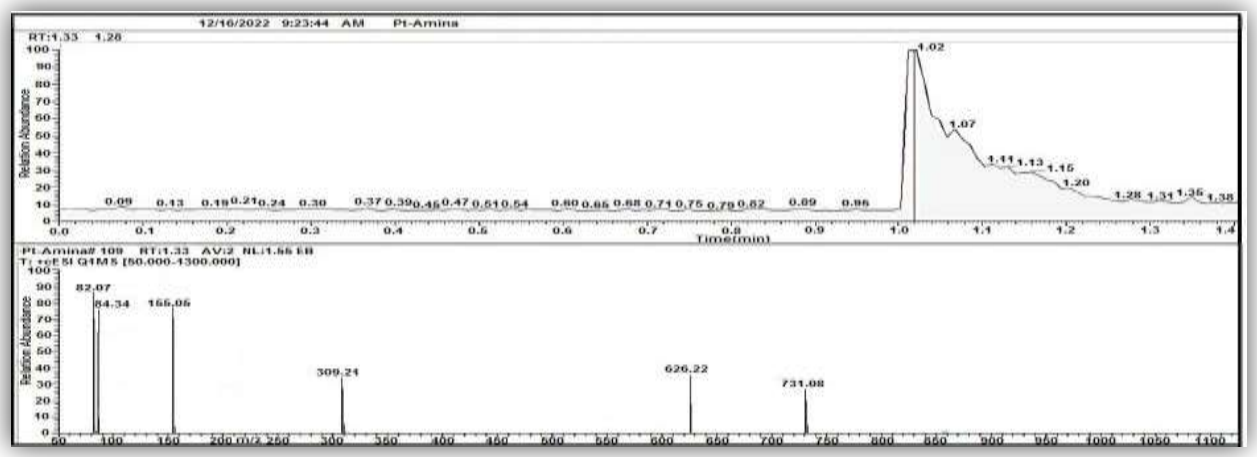

Figue 7. Mass spectrum of Pt-complex.

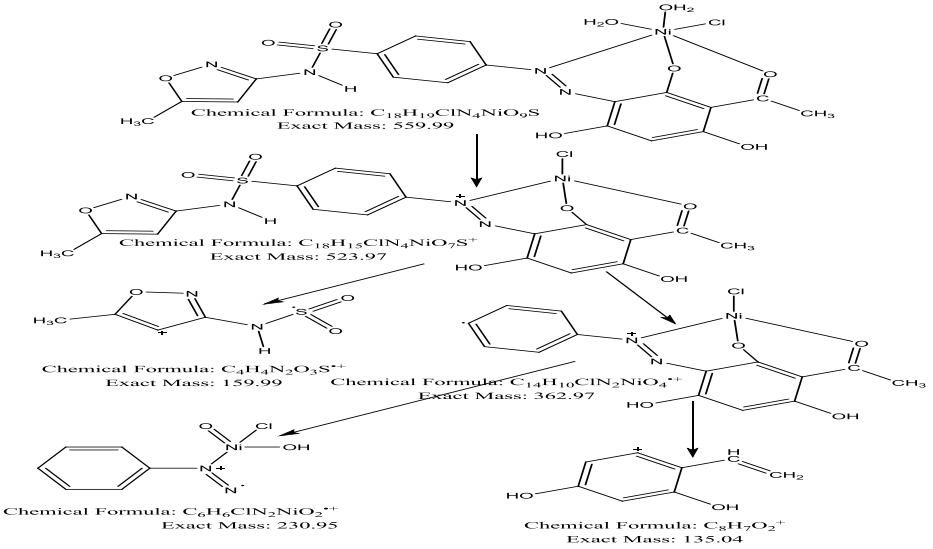

Scheme 3. Pattern of fragmentation of Ni-complex.

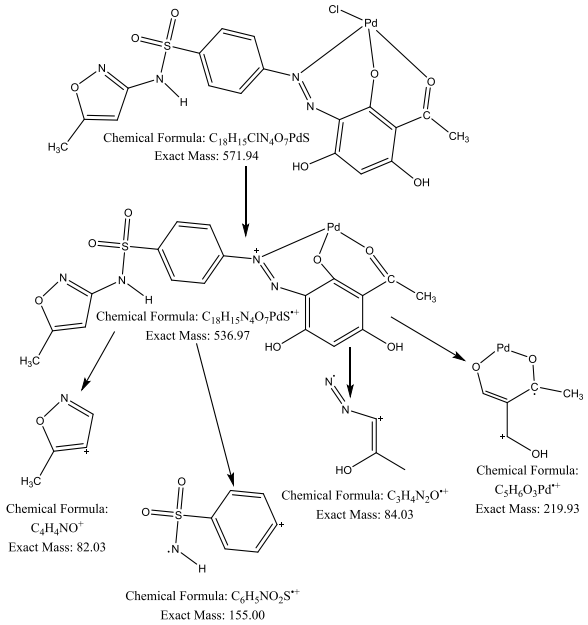

Scheme 4. Pattern of fragmentation of Pd-complex.

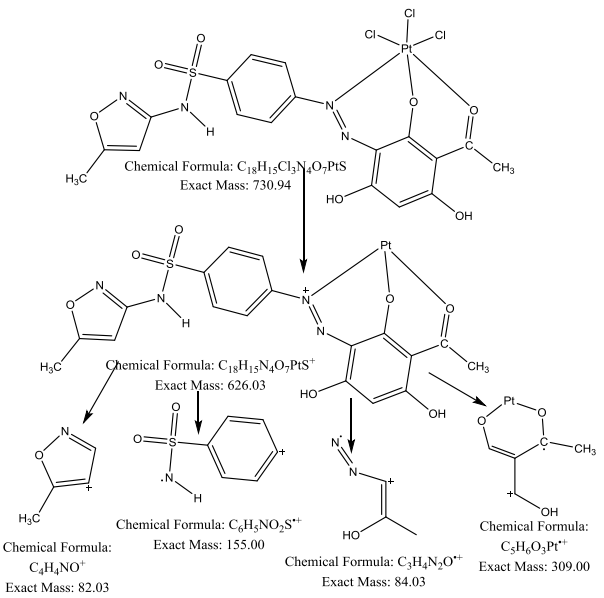

Scheme 5. Pattern of fragmentation of Pt-complex.

Table 3. The LC-Mass spectral data for complexes.

Fragment	m/z Exact mass	Relative Abundance (%)
$[C_{18}H_{19}ClN_4NiO_9S]$	559.99	10
$[C_{18}H_{15}ClN_4NiO_7S]^+$	523.97	47
$[C_{14}H_{10}ClN_2NiO_4]^{\bullet+}$	362.97	65
$[C_6H_6ClN_2NiO_2]^{\bullet+}$	230.95	48
$[C_4H_4N_2O_3S]^{\bullet+}$	159.99	79
$[C_8H_7O_2]^+$	135.04	34
$[C_{18}H_{15}ClN_4O_7PdS]$	571.94	21
$[C_{18}H_{15}N_4O_7PdS]^{\bullet+}$	536.97	11
$[C_5H_6O_3Pd]^{\bullet+}$	219.93	40
$[C_6H_5NO_2S]^{\bullet+}$	155.00	48
$[C_3H_4N_2O]^{\bullet+}$	84.03	35
$[C_4H_4NO]^+$	82.03	34
$[C_{18}H_{15}Cl_3N_4O_7PtS]$	730.94	29
$[C_{18}H_{15}N_4O_7PtS]^+$	626.03	36
$[C_5H_6O_3Pt]^{\bullet+}$	309.00	35
$[C_6H_5NO_2S]^{\bullet+}$	155.00	77
$[C_3H_4N_2O]^{\bullet+}$	84.03	76
$[C_4H_4NO]^+$	82.03	87

3.4 Infrared spectra measurements

The infrared spectra of metal complexes were recorded with Ni^{2+}, Zn^{2+}, Pd^{2+} and Pt^{4+} have been compiled, show in **Figure 8** for Zn complex, **Figure 9** for Pd complex and the data has been organized in **Table 4**. The infrared spectrum of metal complexes showed the vibration frequencies of the double bond N=N; this band suffered a remarkable change in shape, intensity, and position in the spectra of the chelate complexes, which indicates the intercalation of the electron pair of the nitrogen atom of the azo bridge group in the coordination process where N=N and C=O shift, OH disappears and OH water bands appear in addition to the emergence of new packages called the coordination process, which are M-N, M-O and M-Cl. After this, the IR spectra of all produced compounds revealed that the azo-dye ligand connected to metal ions through two sites: the azo group's nitrogen site, and oxygen site via deprotonation of of one of the hydroxyl groups of the aromatic ring [28].

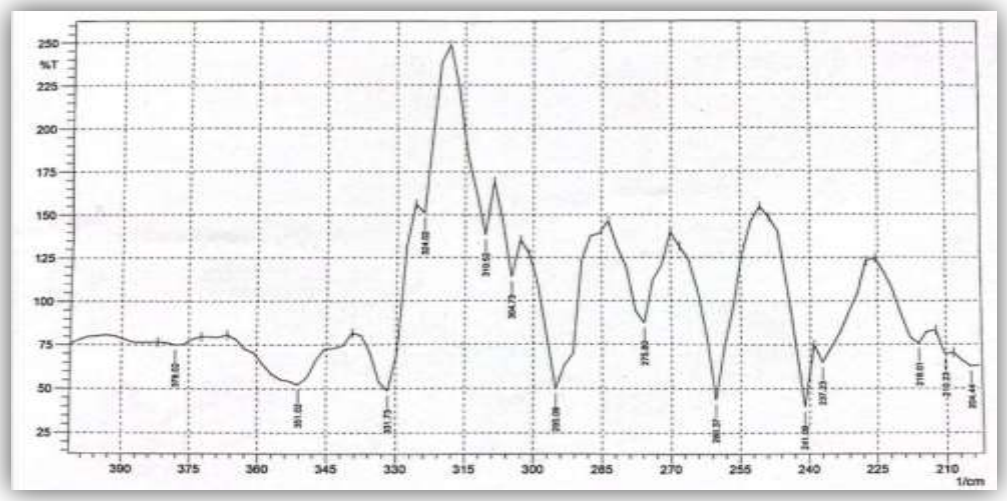

Figure 8. The FT-IR spectrum of Zn-complex.

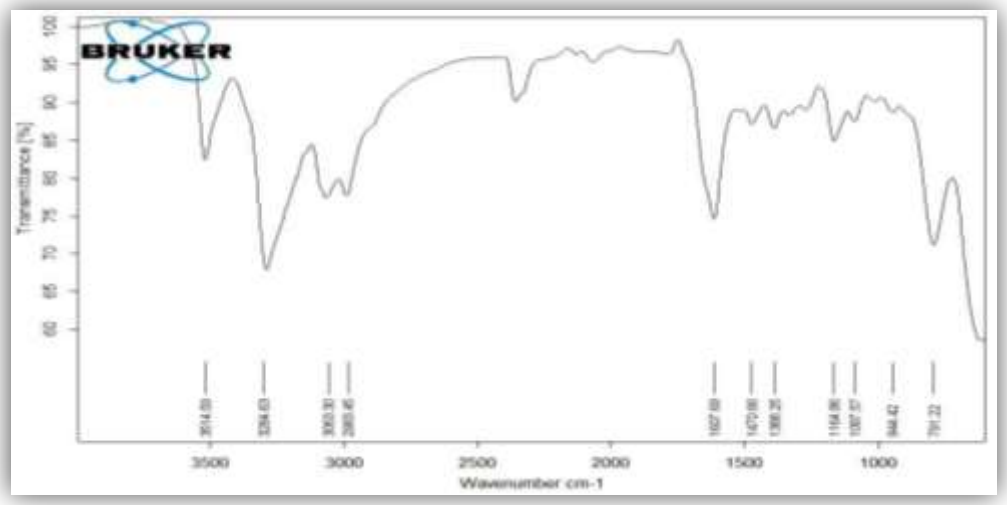

Figure 9. The FT-IR spectrum of Pd-complex.

Table 4. The IR spectral data (cm^{-1}) of complexes.

Compounds	ν (H_2O) aqua	ν (OH) phenolic	ν (NH)	ν (C-H) aromatic aliphatic	N (C=O)	ν (N=N)	ν (SO_2)	M-N M-O M-Cl
$[Ni(H_2L)(H_2O)_2Cl]$	3757	3506	3287	3067 2980	1612	1471	1088 1008	507 459 369
$[Zn(H_2L)(H_2O)Cl]$	3739	3503	3281	3061 2979	1633	1467	1088 1015	528 403 331
$[Pd(H_2L)Cl]$	_	3514	3284	3063 2983	1607	1470	1087	510 433 370
$[Pt(H_2L)Cl_3]$	_	3489	3289	3057 2978	1608	1470	1094 1009	514 405 324

3.5 Thermalstudy data

The results obtained for the thermal analysis for ligand (H_3L) and their synthesized complexes were displayed in **Tables 5** and **6**, and **Figures 10-13** respectively. Tentative decomposition reaction of metal complexes summarize in **Schemes 6**. Decomposition stages, temperature ranges, decomposition products, and weight loss complex percentages were computed based on the thermograms, and they showed agreement. Between their thermal decomposition results and calculated values, that validates elemental analysis results and suggested equations [29]. In this work, it was noted that the remaining ligand was carbon and the remaining metal oxide in the ligand and metal complexes of Ni^{2+}, Pd^{2+} and Pt^{4+}. According to the results of the thermo gravimetric tests, the complexes and the ligand decompose in (1 to 4) phases. The thermodynamic parameters ΔH, ΔS and ΔG were computed using the DCS curve.

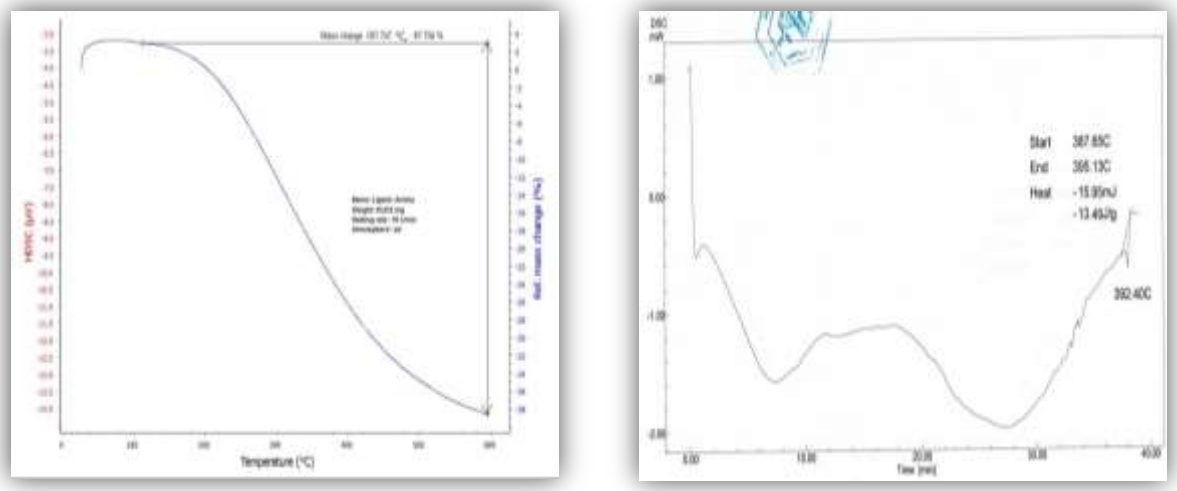

Figure 10. The TGA and DSC curve of ligand (H_3L).

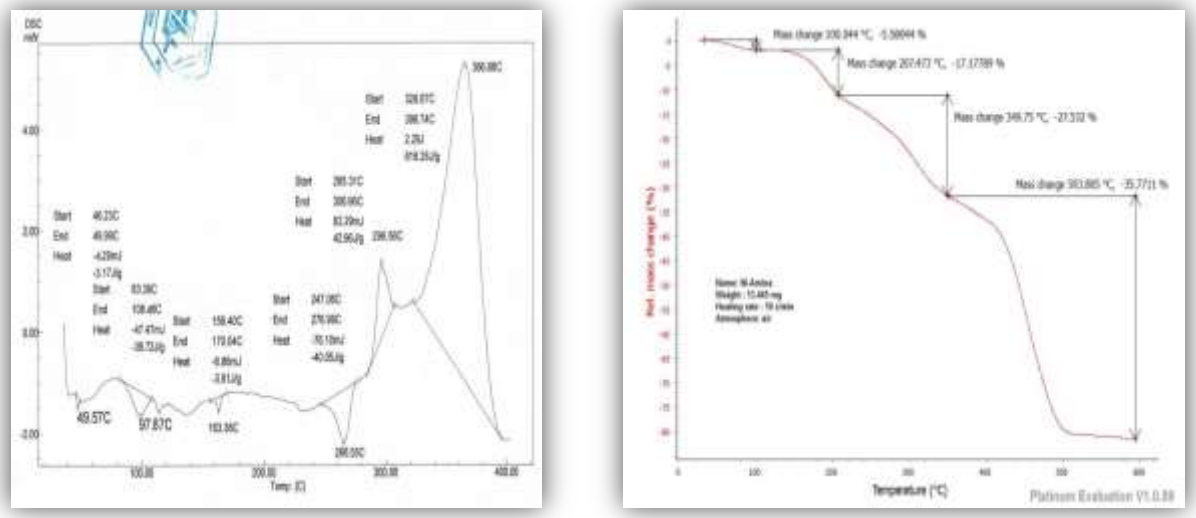

Figure 11. The TGA and DSC curve of Ni-complex.

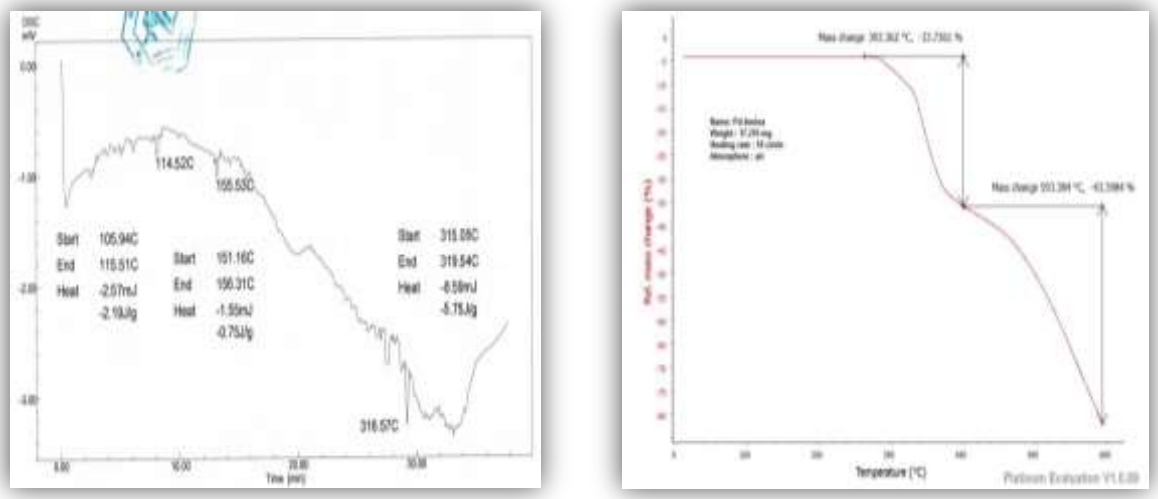

Figure 12. The TGA and DSC curve of Pd-complex

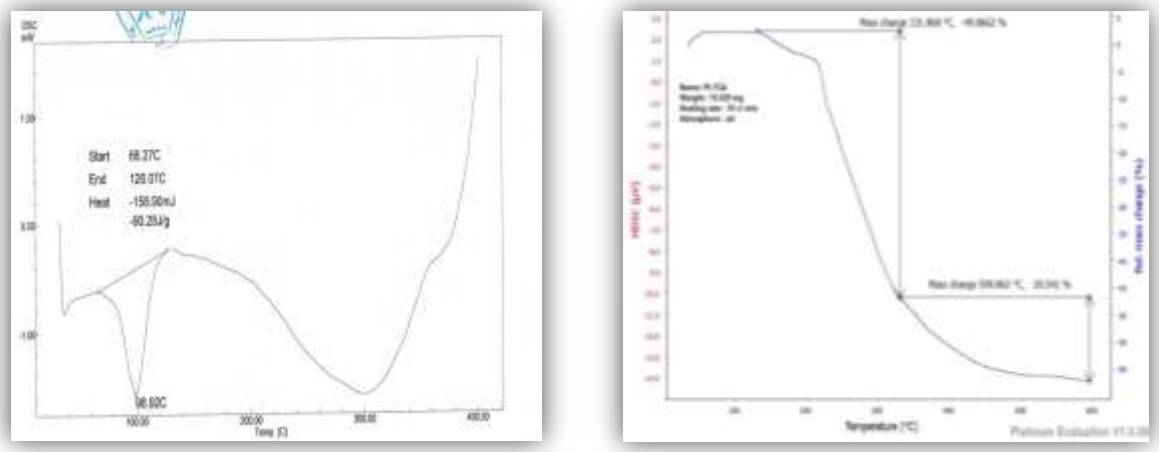

Figure 13. The TGA and DSC curve of Pt-complex.

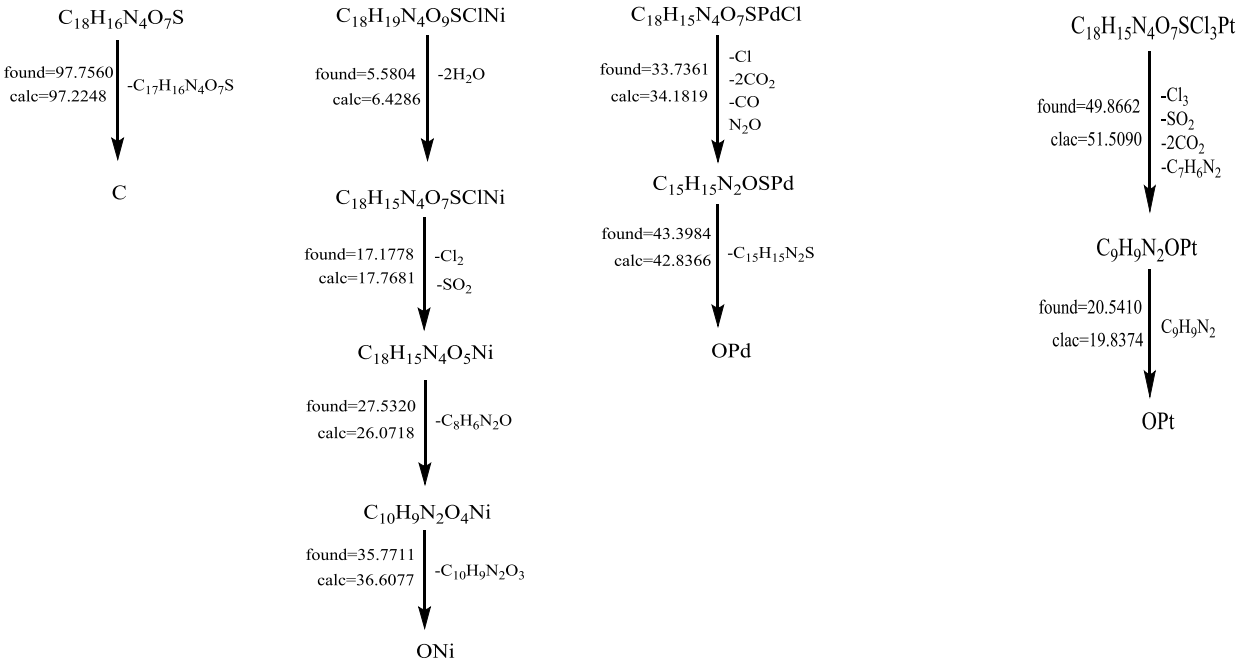

Scheme 6. Tentative decomposition reaction of ligand and metal complexes.

Table 5. The TGA data of the ligand H_3L and some complexes.

Complexes	Step	T_i/°C	T_f/°C	Tmax	Weight mass loss% Calc	Found	Reaction
Ligand	1	111.021	597.747	347.362	97.2248	97.7560	$-C_{17}H_{16}N_4O_7S$ C
		Calculated:97.2248%final=2.7752%;Estimated97.7560%final=2.244%					
Ni-complex	1	32.102	100.044	76.362	6.4286	5.5804	$-2H_2O$
	2	100.011	207.473	149.952	17.7681	17.1778	-Cl, $-SO_2$
	3	208.223	349.75	288.764	26.0718	27.5320	$-C_8H_6N_2O$
	4	350.412	593.805	480.362	36.6077	35.7711	$-C_{10}H_9N_2O_3$ ONi
		Calculated:86.8762% final =13.1238%;Estimated 86.0613% final =13.9387%					
Pd-complex	1	268.200	393.362	301.762	34.1819	33.7361	-Cl,$-2CO_2$,-CO,N_2O
	2	402.998	593.384	476.453	42.8366	43.3984	$-C_{15}H_{15}N_2S$ OPd
		Calculated:77.0185% final =22.9815%;Estimated 77.1345% final =22.8655%					
Pt-complex	1	132.111	331.868	207.936	51.5090	49.8662	$-Cl_3$,$-SO_2$,-$2CO_2$, -C7H6N2
	2	331.001	590.862	461.395	19.8374	20.5410	$-C_9H_9N_2$ OPt
		Calculated:71.3464% final =28.6536%;Estimated 70.4072% final =29.5928%					

Table 6. Thermal decomposition DSC of ligand and some complexes.

Compound	T_i/°C	T_f/°C	Maximum temperature point °C	ΔH J/mol	ΔS J/K.mol	ΔG J/mol	Type
L_3H	387.65	395.13	392.40	-13.49	-1.804	694.399	endothermic
$[Ni(H_2L)(H_2O)_2Cl]$	46.23	49.99	49.57	-3.17	-0.8431	38.6225	endothermic
	83.39	108.46	97.87	-39.72	-1.5844	115.3452	endothermic
	156.40	170.04	163.36	-3.61	-0.2647	39.6314	endothermic
	247.06	276.99	266.55	-40.05	-1.3381	316.6206	endothermic
	285.31	306.96	296.56	42.96	1.9843	-545.504	exothermic
	326.67	396.74	366.66	616.28	8.7952	-2608.568	exothermic
$[Pd(H_2L)Cl]$	105.94	115.51	114.52	-2.19	-0.2288	24.0122	endothermic
	151.16	156.31	155.53	-0.75	-0.1456	21.8952	endothermic
	315.05	319.54	316.57	-5.75	-1.2806	399.6495	endothermic
$[Pt(H_2L)Cl_3]$	66.27	126.07	98.92	-90.28	-1.5097	59.0595	endothermic

3.6 Investigation of antioxidant activity

The assay was used to determine how well antioxidants can scavenge it. Antioxidants provide a hydrogen atom to1-(2,4,6-trihydroxy-phenyl)-ethanone, which reduces the single electrons from nitrogen atoms in DPPH. When the DPPH radical solution is combined with the antioxidant, the color of the corresponding hydrazine changes from violet to yellow, which is characterized by an absorption band in an ethanol solution centered at approximately (517 nm). Electron delocalization also produces dark purple [30]. The interaction of $[Ni(H_2L)(H_2O)_2Cl]$, $[Zn(H_2L)(H_2O)Cl]$,$[Pd(H_2L)Cl]$ and $[Pt(H_2L)Cl_3]$ complexes with DPPH radicals and subsequent hydrogen donation to scavenge the radicals were displayed with **Table 7**. Effective DPPH radical scavenging is indicated by a lower IC_{50} value. In the DPPH assay, the practically Pt-complex has more antioxidant activity than the othermetal complexes [31,32].

Table 7. Antioxidant activity of azo dye and its complexes.

Compounds	Mean	Standard deviation	Coefficient of variation%	Correlation coefficient	IC_{50}(M)
GA	93.5600	2.0846	12.2281	0.9993	6.1135
H_3 L	85.7600	3.0663	13.3521	0.9938	4.6630
$[Ni(H_2L)(H_2O)_2Cl]$	68.8311	4.2753	13.1762	0.9988	3.1625
$[Zn(H_2L)(H_2O)Cl]$	65.4423	3.8123	17.6531	0.9991	4.0109
$[Pd(H_2L)Cl]$	83.1152	3.3796	15.5221	0.9981	3.0025
$[Pt(H_2L)Cl_3]$	71.3217	2.2009	14.4119	0.9975	2.704

4. Conclusion

In summary, this study has successfully synthesized a new azo ligand derivative of sulfamethoxazole by simple substitution reaction with 1-(2,4,6-trihydroxy-phenyl)-ethanone. Then characterized ligand and metal complexes by various analytical techniques, like elemental microanalysis, metal–chloride containing, electrical conductivity measurement, magnetic susceptibility,^{1}H and ^{13}CNMR, FT-IR,UV-Vis , mass spectroscopy, and thermal analysis (TGA and DSC) curves. The DCS curve was used to calculated the thermodynamic parameters ΔH, ΔS, and ΔG.The yield of the synthesized compounds was found to be in the range from 60-80%.The molar conductivity results showed that none of the produced complexes are electrolytes, and the atomic N, O and O tridentate coordination sites in the ligand were identified by comparing their IR spectra to those of the metal complexes. The M:L ratio in every compound was [1:1]. According to the results, Octahedral geometry suggests (Ni^{2+} and Pt^{4+}), Tetrahedral of Zn^{2+} complex, and Square planer of Pd^{2+}. The antioxidant activity of the synthetic compounds was evaluated against the DPPH radical (1.1-diphenyl-2-picrylhydrazyl), and the results were contrasted with those of gallic acid, a widely used natural antioxidant. Results show how efficient metal complexes are in scavenging free radicals.

Acknowledgment

The authors would like to thank everyone who contributed to the success of this review article. Department of Chemistry, College of Science for Women, Baghdad University, Prof. Dr. Abbas Ali Salih Al-Hamdani, Ministry of Higher Education & Scientific Research and Ministry of Science and Technology, Directorate of Environment and Water.

Conflict of Interest

None

Funding

There is no financial support.

Ethical Clearance

This work has been approved by the Scientific Committee at the University of Baghdad/ College of Science for Women.

References

1. Al-Hamdani, A.A.S.; Balkhi, A.M., Shaker, A.F.S.A. Synthesis and investigation of thermal properties of vanadyl complexes with azo-containing Schiff-base dyes. *Journal of Saudi Chemical Society* **2016**, *20(5)*, 487-501. https://doi.org/10.1016/j.jscs.2012.08.001.
2. Resheed, F.A.; AL-Hamdani, A.A.S.; Abdullah, S.M. Green synthesis zinc nanoparticles in the treatment of heavy metals in the form of complexes. *Ibn Al-Haitham Journal For Pure and Applied Sciences* **2023**, *36(3)*,201-213. https://doi.org/10.30526/36.3.3056.
3. Malik, H.; Akhter, Z.; Shahbaz, M.; Yousuf, S.; Munawar, K.S.; Muhammad, S.; Ahmad, T. Synthesis, spectroscopic characterization, single crystal, theoretical investigation, and biological screenings of azo-based moieties. *Journal of Molecular Structure* **2022**, *1270*, 133867. https://doi. 10.1016/j.molstruc.2022.13386.
4. Nagasundaram, N.;Govindhan, C.; Sumitha, S.; Sedhu, N.; Raguvaran, K.; Santhosh, S.; Lalitha, A. Synthesis, characterization and biological evaluation of novel azo fused 2, 3-dihydro-1H-perimidine derivatives: In vitro antibacterial, antibiofilm, anti-quorum sensing, DFT, in silico ADME and Molecular docking studies. *Journal of Molecular Structure* **2022**, *124*,131437. https://doi.org/10.1016/j.molstruc.2021.131437.
5. Al-Daffay, R.K.H.; Al-Hamdani, AAS. Synthesis and characterization of some metals complexes with Nnew acidicazo ligand 4-[(2-Amino-4-Phenylazo)-Methyl]-cyclohexane carboxylic acid. *Iraqi Journal of Science* **2022**,*63(8)*,3264-3275. https://doi.org/10.24996/ijs.2022.63.8.2.
6. Reda, SM.; Al-Hamdani AAS. Synthesis, characterization, thermal analysis and bioactivity of some transition metals complexes with new azo ligand. *Chemical Methodologies* **2022**, *6(6)*, 475-493. https://doi.org/10.22034/chemm.2022.335815.1468.
7. Al-Daffay, R.K.; Al-Hamdani, AA. Synthesis, Characterization, and thermal analysis of a new acidic azo ligand's metal complexes. *Baghdad Science Journal* **2022**, *19(3)*,121-133. https://doi.org/10.21123/bsj.2022.6709.
8. Al Zoubia, W.; Al-Hamdani, AAS.; Kaseem, M. Synthesis and antioxidant activities of Schiff bases and their complexes: A review. *Applied Organometallic chemistry* **2016**, *30(10)*,810-817. https://doi.org/10.1002/aoc.3506.
9. Samy, M.E.; Moamen S.R.; Fawziah A.A.;Reham Z.H. Situ neutral system synthesis, spectroscopic, and biological interpretations of magnesium(II), calcium(II), chromium(III), zinc(II), copper(II) and selenium (IV) sitagliptin complexes. *Int J Environ Res Public Health* **2021**, *18(8030)*,1-19. https://doi. 10.3390/ijerph18158030.
10. Al Zoubi, W.; Al-Hamdani, A.A.S.; Ko, Y.G. Schiff bases and their complexes:Recent progress in thermal analysis. *Separation Science and Technology* **2017**, *52(6)*,1052-1069. https://doi.10.1080/01496395.2016.1267756.
11. Al Zoubi, W.; Al-Hamdani, A.A.S., Widiantara, I.P.; Hamoodah, R.G.; Ko,Y.G. Theoretical studies and antibacterial activity for Schiff base complexes. *Journal of Physical Organic Chemistry* **2017**, *30(6)*, e3707. https://doi. 10.1002/poc.3707.
12. Al Zoubi, W.; Al-Hamdani, A.A.S.; Ahmed, S.D.; Ko, Y.G. Synthesis, characterization, and biological activity of schiff bases metal complexes. *Journal of Physical Organic Chemistry* **2018**, *31(2)*,e3752. https://doi. 10.1002/poc.3752.
13. Abdulrazzaq, A.G.; Al-Hamdani, A.A.S. Cr (III), Fe (III), Co (II) and Cu (II) metal ions complexes with azo compound derived from 2-hydroxy quinolin synthesis, characterization, thermal study and antioxidant activity. *Ibn AL-Haitham Journal For Pure and Applied Sciences* **2023**, *36(3)*,214-230. https://doi.org/10.30526/36.3.3068.
14. Obaid, S.M.H.; Jarad, A.J.; Al-Hamdani, A.A.S. Synthesis, characterization and biological activity of mixed ligand metal saltscomplexes with various ligands. *Journal of Physics: Conference Series* **2020**, *1660(1)*,12028. https://doi.10.1088/1742-6596/1660/1/012028.

15. Keshavayya, J.; Pushpavathi, I.; Keerthikumar, C.T.; Maliyappa, M.R.;Ravi, B.N. Synthesis, characterization, computational and biological studies of nitrothiazole incorporated heterocyclic azo dyes. *Journal of Structural Chemistry* **2020**, *31(4)*,1317-1329. https://doi.10.1007/s11224-020-01493-0.
16. Moamen, S.R., Altalhi, T.; Safyah, B.B.; Ghaferah, H.A.; Kehkashan, A. New Cr(III), Mn(II), Fe(III), Co(II), Ni(II), Zn(II), Cd(II),and Hg(II) gibberellate complexes: Synthesis, structure, and inhibitory activity against COVID-19 protease. *Russian Journal of General Chemistry* **2021**, *91(5)*, 890-896. https://doi.10.1134/S1070363221050194.
17. Jirjees, V.Y.; Al-Hamdani, A.A.S.;Wannas, N.M.; Abdall, F.R.; Dib, A.; Al Zoubi, W. Spectroscopic characterization for new model from Schiff base and its complexes. *Journal of Physical Organic Chemistry* **2021**, *34(4)*,e4169. https://doi.org/10.1002/poc.4169.
18. Abdullah, S.M.; Al-Hamdani, A.A.S.; Ibrahim, S.M.; Al-Zubaid, L.M.; Rashid, F.A. An evaluation of activity of prepared zinc nanoparticles with extract green plant in treatments of diclofenac, levofloxacin, and tetracycline in water. *Journal of Medicinal and Chemical Sciences* **2023**, *6(6)*,1323-1335. https://doi.org/10.26655/JMCHEMSCI.2023.6.12.
19. Maliyappa, M.R..;Keshavayya, J.; Mallikarjuna, N.M.; Krishna, PM.; Shivakumara, N.; Sandeep, T.; Nazrulla, M.A. Synthesis, characterization, pharmacological and computational studies of 4, 5, 6, 7-tetrahydro-1,3-benzothiazole incorporated azo dyes. *Journal Molecular Structure*, **2019**, *1179*, 630-641. https://doi.10.1016/j.molstruc.2018.11.041.
20. Kareem, M.J.; Al-Hamdani, A.A.S.; Ko, Y.G.; Al Zoubi, W.; Mohammed, S.G. Synthesis, characterization, and determination antioxidant activities for new schiff base complexes derived from 2-(1H-indol-3-yl)-ethylamine and metal ion complexes. *Journal of Molecular Structure* **2023**, *20*, 319827. https://doi.10.1016/j.molstruc.2020.129669.
21. Al Zoubi, W.; Al-Hamdani, A.A.S.; Sunghun, B., Ko, Y.G. A review on TiO_2-based composites for superior photocatalytic activity. *Reviews in Inorganic Chemistry-De Gruyter* **2021**, *234*,108863. https://doi.10.1515/revic-2020-0025.
22. Hamza, I.S.;Mahmmoud, W.A.; Al-Hamdani, A.A.; Ahmed, S.D.; Allaf, A.W.; Al Zoubi, W. Synthesis, characterization, and bioactivity of several metal complexes of (4-Amino-N-(5-methyl-isaxazol-3-yl)-benzenesulfonamide). *Inorganic Chemistry Communications* **2022**, *144*,109776. https://doi.org/10.1016/j.inoche.2022.109776.
23. Al-Hamdani, A.A.S.; Al-Alwany, T.A.M.; Mseer, M.A.; Fadhel, A.M.; Al-Khafaji, Y.F. Synthesis, characterization, spectroscopic, thermal and biological studies for new complexeswith N_1, N_2-bis (3-hydroxyphenyl) oxalamide. *Egyptian Journal of Chemistry* **2022**, *8*,8. https://doi.10.21608/EJCHEM.2022.144403.6297.
24. Kareem, M.J.; Al-Hamdani, A.A.S.; Jirjees, V.Y.; Khan, M.E.; Allaf, A.W.; Al Zoubi, W. Preparation, spectroscopic study of Schiff base derived from dopamine andmetal Ni(II),Pd(II), and Pt(IV) complexes,and activity determination asantioxidants. *Journal of Physical Organic Chemistry* **2020**, e4156. https://doi.10.1002/poc.4156.
25. Reda, S.M.; Al-Hamdani, A.A.S. Mn (II), Fe (III), Co (II) and Rh (III) complexes with azo ligand: Synthesis, characterization, thermalanalysis and bioactivity. *Baghdad Science Journal* **2022**, *133*, 511-523. https://doi.org/10.21123/bsj.2022.7289.
26. Al-Daffay, R.K.H.; Al-Hamdani, A.A.S.; Al Zoubi, W. Synthesis, characterization and thermal analysis of Cu (II), Co (II), Ru(III) and Rh(III) complexes of a new acidic ligand. *Ibn Al-Haitham Journal for Pure and Applied Sciences* **2023**, *36(4)*,321-337. https://doi.org/10.30526/36.4.3047.
27. Obaid, S.M.H.; Sultan, J.S.; Al-Hamdani, A.A.S. Synthesis, characterization and biological efficacies from some new dinuclear metal complexes for base 3-(3,4-dihydroxy-phenyl)-2-[(2-hydroxy-3-methylperoxy-benzylidene)-amino]-2-methyl propionic acid. *Indones Journal of Chemistry* **2020**, *20(6)*, 1311-1322. https://doi.10.22146/ijc.49842.

28. Al-Hamdani, A.A.S.; Al Zoubi, W. New metal complexes of N3 tridentate ligand: Synthesis, spectral studies and biological activity. *Spectrochim Acta A Mol Biomol Spectrosc* **2015**, *137*,75-89. https://doi.10.1016/j.saa.2014.07.057.
29. Al Zoubi, W.; Al-Hamdani, A.A.S; Ahmed, S.D.; Basheer, H.M.; Al-Luhaibi, R.S.; Dib, A.; Ko, Y.G. Synthesis, characterization, and antioxidant activities of imine compounds. *Journal of Physical Organic Chemistry* **2018**, *32*,1-9. https://doi.org/10.1002/poc.3916.
30. Abdulrazzaq A.G., Al-Hamdani, A.A.S. Ni^{2+}, Pt^{4+}, Pd^{2+}, and Mn^{2+} metal ions complexes with azo derived from quinolin-2-ol and 3-amino-N-(5-methylisoxazol-3-yl) benzenesulfonamide: Synthesis, characterization, thermal study, and antioxidant activity. *Baghdad Sciences Journal* **2023**, *20(6)*, 2207-2223. https://doi.org/10.21123/bsj.2023.7708.
31. Al-Hamdani, A.A.S., Abdulridha, M.Q. Synthesis, characterization of new metal complexes of Co(II), Cu(II), Cd(II) and Ru(III) from azo ligand 5- ((2-(1H-indol-2-yl) ethyl) diazinyl)- 2-aminophenol, thermal and antioxidant studies. *Baghdad Science Journal* **2023**, *20(5)*,1964-1975. https://doi.org/10.21123/bsj.2023.7629.
32. Abdulrazzaq, A.G., Al-Hamdani, A.A. SCr (III), Fe (III), Co (II) and Cu (II) metal ions complexes with azo compound derived from 2-hydroxy quinolin synthesis, characterization, thermal study and antioxidant activity. *Ibn AL-Haitham Journal For Pure and Applied Sciences* **2023**, *36(3)*,214-230. https://doi.org/10.30526/36.3.3068.